

# CFD ANALYSIS OF THERMOHYDRODYNAMIC BEHAVIOR OF NANOLUBRICATED JOURNAL BEARINGS CONSIDERING CAVITATION EFFECT

Saba Y. Ahmed, Basim A. Abass\*, Zainab H. Kadhim

University of Babylon, College of Engineering, Mechanical Engineering Department

e-mail: eng.basim.ajeel@uobabylon.edu.iq

\* *corresponding author*

## Abstract

The present work displays an extensive numerical analysis for the thermo-hydrodynamic (THD) behavior in finite length journal bearings lubricated with different types of nano-lubricants considering cavitation effect. The effects of nanoparticle concentrations, cavitation and temperature rise on the performance parameters of such bearings have been explored. The bearing is simulated using Computational Fluid Dynamic (CFD) approach. The effect of using different types of nano-lubricants with different volume fractions of  $\text{TiO}_2$  and  $\text{Al}_2\text{O}_3$  nanoparticles dispersed in Veedol Avalon ISO Viscosity grade 46 oil has been demonstrated. Modified Krieger-Dougherty equation has been implemented with the thermal viscosity model to evaluate the oil effective viscosity. The obtained results show that concerning the  $\text{TiO}_2$  nanoparticles results in a higher oil film pressure and load carrying capacity in comparison with  $\text{Al}_2\text{O}_3$ . The bearing equilibrium position was obtained by using Response Surface analysis (RSA) with optimal space-filling design technique. The numerical model was validated by comparing the results obtained in the present work with that obtained by Feron et al. The results were found to be in a good confirmation. The attained results show that the maximum pressure grows by 21% when the bearing is lubricated with nano-lubricant.

**Keywords:** Hydrodynamic journal bearings, computational fluid dynamics, thermohydrodynamic lubrication, Nano-lubricant, cavitation effect, optimization.

## 1. Introduction

Journal bearing is the most commonly hydrodynamic bearing used to support the rotating shafts in industrial machines due to its simplicity and low costs. It is mainly used to support the externally applied load due to the generated pressure in its oil film. This type of bearings suffers from instability when it works at high speeds. The oil film temperature increases due to the viscous shearing of the oil film resulting in a decrease in the oil viscosity which negatively affects the performance of the bearing. Also, the oil film pressure drops at the divergent part of the bearing and when it becomes below than the saturation pressure the dissolved air bubbles released leading to the cavitation phenomenon. The reliable analysis of the bearing performance needs considering the effects of all the above parameters. Lubricant can be improved potentially by adding nanoparticles. Their nanometer scale allows them to pass the contact area easily. Many

researchers studied the performance of journal bearing lubricated with nano-lubricants considering different parameters such as thermal and cavitation effects using CFD or other conventional techniques. The temperature field in cylindrical journal bearing lubricated with pure oil was studied extensively by different workers using CFD, conjugate and convection heat transfer approaches Singla et al. (2014), Han et al. (2017), and Li et al. (2018). Binu et al. (2014) discussed the effect of TiO<sub>2</sub> nanoparticles added to the lubricant the load carried by the bearing. It was found that the viscosity of the lubricant increases due to presence of TiO<sub>2</sub> nanoparticles which were modeled using a modified Krieger-Dougherty model. The static performance of thermo-hydrodynamic journal bearings operating under different types of lubricants dispersed with different types of nano-particles have been studied extensively (Nair et al. 2011; Binu et al. 2014; Babu et al. 2014; Kalakada 2015; Kumar 2017; Jamalabadi 2019). Different works have been implemented to study the static performance characteristics of journal bearings lubricated with oil dispersed with different nanoparticles. Awati and Kengangutti (2018) presented the effect of surface roughness on the static performance characteristics of thermo-hydrodynamic journal bearing operating under nano-lubricants. Different types of nanoparticles have been used such as CuO, CeO<sub>2</sub>, and Al<sub>2</sub>O<sub>3</sub>. Suryawanshi and Pattiwar(2018) analyzed plain and elliptical journal bearings performance work under industrial lubricants dispersed with titanium dioxide nanoparticle of size 40 nm. Suryawanshi and Pattiwar(2019) studied the performance characteristics of the journal bearing with different geometries lubricated with different types of oil dispersed with TiO<sub>2</sub> nanoparticles experimentally. Singh et al. (2020) analyzed the performance of journal bearing lubricated with commercial SAE30 lubricant dispersed with different volume fractions of TiO<sub>2</sub> nanoparticles. Ramaganesh et al. (2020) used COMSOL multiphysics software to analyze the performance of journal bearing lubricated with different nanolubricants. The suitability of the model used was validated with the experimental results. Gundarneeeya and Vakharia (2021) analyzed the performance of journal bearing lubricated with Avalon ISO Viscosity grade 46 containing TiO<sub>2</sub>, CuO and Al<sub>2</sub>O<sub>3</sub> nanoparticles as an additives. Dang et al. (2021) optimized the equipment efficiency to improve the performance of the circular journal bearings lubricated with TiO<sub>2</sub> and CuO nanolubricants. The effect of using different bio-lubricants dispersed with different types of Nano-particles on the performance of conventional journal bearing numerically and experimentally was studied in different works. Katpatal et al. (2019) examined the effect of using different bio lubricants dispersed with CuO nanoparticles on the performance of hydrodynamic journal bearings experimentally. It is found that the oil film pressure is mainly dependent on the viscosity of such lubricants. Dhanola and Garg(2020) studied the thermal behavior of a journal bearing lubricated with nano-bio-based oil using adiabatic solutions. The oil film pressure and temperature distributions had been evaluated by numerical solution of the Reynolds and the adiabatic energy equations. The cavitation effect on the journal bearing performance was also considered in different research works. Rasep et al.(2021)compared the performance of the journalbearing with and without cavitation using CFD technique. The effect of using different types of lubricants such as palm oil, and engine oil (SAE40W) were studied. Alakhramsing et al. (2015) used mass conserving cavitation algorithm to implement thermo-hydrodynamic analysis of a Plain Journal bearing. Sakai et al.(2017) analyzed the cavitation area in small-bore journal bearing under flooded and starved lubrication using CFD technique while the two-phase flow was analyzed using volume of fluid (VOF) method. The effect of setting conditions of VOF such as surface tension, and vapor pressure were studied and the results were compared with that obtained experimentally. Sadabadi and Nezhad (2020)used discrete phase modeling (DPM) with computational fluid dynamic approach to study the effect of IF-WS2 nano-lubricant on the load carried by the journal bearing. Dang et al.(2021) examined the consequence of using TiO<sub>2</sub> and CuO based Nano-lubricants on the static behavior of journal bearings considering thermal effect. The main purpose of the present work is to simulate the thermo-hydrodynamic performance of a full journal bearing lubricated with different Nano-lubricants considering cavitation effect which is rarely studied previously.

## 2. Mathematical model

### 2.1 Governing equations

The static characteristics of nano-lubricated plain journal bearing shown in Figure 1 with the geometrical and physical properties shown in Table 1 is conducted by using computational fluid dynamic (CFD) algorithm via ANSYS-FLUENT 19.2 software.

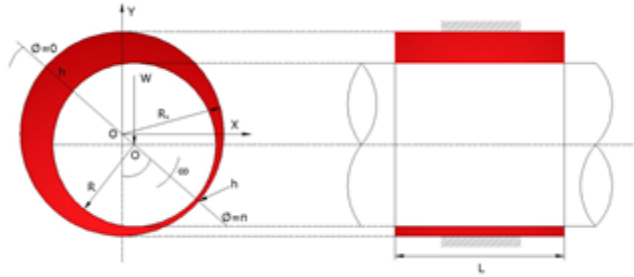


**Fig. 1.** Journal bearing (Dhande (2017)).

Parameter	Symbol	Value
Aspect Ratio	$L/D$	0.5
Shaft radius	$R_s$	24.95 mm
Bearing Inner radius	$R_i$	25mm
Bearing outer radius	$R_o$	30 mm
Eccentricity ratio	$\varepsilon$	0.1-0.9
Attitude angle	$\phi$	$49^\circ$
Journal speed	$N$	3000 rpm
Bearing inlet temp.	$T_i$	$40^\circ\text{C}$
Radial clearance	$C$	0.05mm
Oil viscosity at $T_i$ °C	$\mu_o$	0.0788 Pa.s
Viscosity-Temp. coef.	$\beta$	$0.032^\circ\text{C}^{-1}$
Oil density	$\rho_{oil}$	$875 \text{ kg/m}^3$
Oil heat capacity	$C_{Poil}$	$2000 \text{ J/kg }^\circ\text{C}$
Oil thermal conductivity	$k_{oil}$	$0.13 \text{ W/m.}^\circ\text{C}$
Oil vapor pressure	$P_v$	29185 Pa
Volume fraction	$\phi$	0-3%

**Table 1.** Geometrical properties of the bearing (Dhande and Pande (2017)).

The governing equations required to obtain the oil film pressure and temperature can be expressed as:

Continuity equation (Malalasekera (2007))

$$\frac{\partial \rho}{\partial t} + \frac{\partial u}{\partial x} + \frac{\partial v}{\partial y} + \frac{\partial w}{\partial z} \quad (1)$$

Three-dimensional momentum equations

Momentum in x-direction (Malalasekera (2007))

$$\rho \frac{Du}{Dt} = -\frac{\partial p}{\partial x} + \frac{\partial}{\partial x} \left[ 2\mu \frac{\partial u}{\partial x} + \lambda \text{div}u \right] + \frac{\partial}{\partial y} \left[ \mu \left( \frac{\partial u}{\partial y} + \frac{\partial v}{\partial x} \right) \right] + \frac{\partial}{\partial z} \left[ \mu \left( \frac{\partial u}{\partial z} + \frac{\partial w}{\partial x} \right) \right] + S_{Mx} \quad (2)$$

Momentum in y-direction, (Malalasekera (2007))

$$\rho \frac{Dv}{Dt} = -\frac{\partial p}{\partial y} + \frac{\partial}{\partial x} \left[ \mu \left( \frac{\partial u}{\partial y} + \frac{\partial v}{\partial x} \right) \right] + \frac{\partial}{\partial y} \left[ 2\mu \frac{\partial v}{\partial y} + \lambda \text{div}v \right] + \frac{\partial}{\partial z} \left[ \mu \left( \frac{\partial v}{\partial z} + \frac{\partial w}{\partial y} \right) \right] + S_{My} \quad (3)$$

Momentum in z-direction

$$\mu_i = \mu_o \left( 1 - \frac{\varphi_a}{\varphi_m} \right)^{-2.5\varphi_m} \quad (4)$$

where

$$\begin{aligned} S_{Mx} &= \left[ \frac{\partial}{\partial x} \left( \mu \frac{\partial u}{\partial x} \right) + \frac{\partial}{\partial y} \left( \mu \frac{\partial v}{\partial x} \right) + \frac{\partial}{\partial z} \left( \mu \frac{\partial w}{\partial x} \right) \right] \\ S_{My} &= \left[ \frac{\partial}{\partial x} \left( \mu \frac{\partial u}{\partial y} \right) + \frac{\partial}{\partial y} \left( \mu \frac{\partial v}{\partial y} \right) + \frac{\partial}{\partial z} \left( \mu \frac{\partial w}{\partial y} \right) \right] \\ S_{Mz} &= \left[ \frac{\partial}{\partial x} \left( \mu \frac{\partial u}{\partial z} \right) + \frac{\partial}{\partial y} \left( \mu \frac{\partial v}{\partial z} \right) + \frac{\partial}{\partial z} \left( \mu \frac{\partial w}{\partial z} \right) \right] \end{aligned} \quad (5)$$

The temperature of the oil film can be expressed by solving the following three-dimensional energy equation (Malalasekera(2007)).

$$\rho C_p \left( u \frac{\partial T}{\partial x} + w \frac{\partial T}{\partial z} \right) = \frac{\partial}{\partial y} \left( k \frac{\partial T}{\partial y} \right) + \mu \left[ \left( \frac{\partial u}{\partial y} \right)^2 + \left( \frac{\partial w}{\partial y} \right)^2 \right] \quad (6)$$

The steady state condition for laminar flow of lubricant film was assumed neglecting the body forces. The flow of the lubricant in the cavitation zone can be modeled by the following equation (Dhande (2017)):

$$\frac{\partial}{\partial t} (a_v \cdot \rho_v) + \nabla (a_v \cdot \rho_v \cdot v_v) = N_e - N_c \quad (7)$$

According to Zwart–Gerber–Balamri cavitation model:

$$\begin{aligned}
 & \text{if, } p < p_v \\
 N_e &= F_{evap} \cdot \frac{3a_{nue} (1 - a_v) \rho_v}{R_b} \sqrt{\frac{2}{3} \cdot \frac{p_v - p}{\rho l}} \quad (8)
 \end{aligned}$$

$$\begin{aligned}
 & \text{f, } p \geq p_v \\
 N_c &= F_{cond} \frac{3a_v \rho_v}{R_b} \sqrt{\frac{2}{3} \cdot \frac{p - p_v}{\rho l}} \quad (9)
 \end{aligned}$$

$R_b$  is the radius of the bubble which can be described by Rayleigh-Plesset equation (Dhande (2017)):

$$\frac{dR_b}{dt} = \sqrt{\frac{2}{3} \cdot \frac{p_b - p}{\rho l}} \quad (10)$$

The effect of the oil film temperature on the viscosity of the Nano-lubricant can be considered by using the following equation (Mishra et al.2014):

$$\mu = \mu_{i,f} e^{-\beta(T - T_{in})} \quad (11)$$

where:

$$\mu_i = \mu_o \left( 1 - \frac{\varphi_a}{\varphi_m} \right)^{-2.5\varphi_m} \quad (12)$$

$\varphi_m$  the highest particle packing fraction, which ranges between 0.495 to 0.54 it is around 0.605 for high shear rates.  $\mu_o$  is the pure oil viscosity at the inlet temperature:

$$\varphi_a = \varphi \left( \frac{a_a}{a} \right)^{3-D} \quad (13)$$

$\varphi$  volume fraction of the nanoparticles,  $D$  represents the fractal index for nanofluids with a standard value of 1.8,  $\frac{a_a}{a}$  represents the radii of aggregate to primary particle size ratio. Experimental values for aggregate ratio obtained in reference (Tushar and Vakharia (2021)) are adopted in the present work. Hence, the aggregate ratios of 4,3.33 and 3.5 are adopted for  $\text{TiO}_2$ ,  $\text{Al}_2\text{O}_3$  and  $\text{CuO}$  respectively. Equation (11) can be rewritten as (Mishra (2014)):

$$\mu = \mu_o \left( 1 - \frac{\varphi_a}{\varphi_m} \right)^{-2.5\varphi_m} e^{-\beta(T - T_{in})} \quad (14)$$

$\beta$  is oil viscosity coefficient which can be taken as 0.032.

The other physical and thermal properties of the lubricant can be expressed as (Solghar (2015)):

$$\rho_{nf} = (1 - \varphi)\rho_f + \varphi\rho_p \quad (15)$$

$$\rho_{nf} C_{pnf} = (1 - \varphi)(\rho C_p)_f + \varphi(\rho C_p)_p \quad (16)$$

$$k_{nf} = k_f \left[ \frac{(k_p - 2k_f) - 2\varphi(k_f - k_p)}{(k_p + 2k_f) + \varphi(k_f - k_p)} \right] \quad (17)$$

where  $\rho_{nf}$ ,  $\rho_{nf}$  and  $k_{nf}$  are the density, the heat capacity and the thermal conductivity of the nano-lubricant respectively.

## 2.2 Boundary conditions

The conservation and energy equations are solved with the following boundary conditions to obtain the distribution of the oil film temperature: The oil inlet pressure and temperature are taken as 0.2Mpa (equal to supply pressure) and 313K. The pressure at both ends of the bearing was taken as an ambient pressure as can be observed from Figure 2. The oil temperature at the bearing outlet was taken as 300K. The outer surface of the rotating journal and the inner surface of stationary bearing are coupled with the oil film. Coherent boundary condition was adopted which stated that the oil velocity takes the values of surface velocities with no-slip boundary condition.

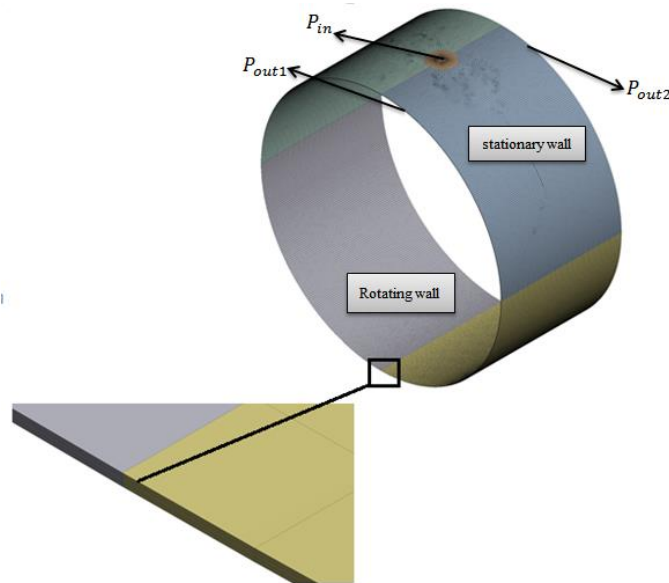


**Fig. 2.** Fluid film boundary conditions.

## 2.3 Bearing Performance Parameters

The load components in x and y directions can be calculated as (Dhande and Pande (2017)):

$$F_x = \iint_{A_j} P_j \sin \theta (dA_j) \quad (18)$$

$$F_y = \iint_{A_j} P_j \cos \theta (dA_j) \quad (19)$$

The load carried by the bearing can be calculated as (Dhande and Pande (2017)):

$$W = \sqrt{(F_x)^2 + (F_y)^2} \quad (20)$$

The attitude angle of the bearing can be calculated as (Dhande and Pande (2017)):

$$\phi = \tan^{-1} \left( \frac{F_y}{F_x} \right) \quad (21)$$

#### 2.4 CFD model

The oil film is meshed and modeled by using FLUENT software. The oil film is discretized to 133767 hexahedral finite volume with 0.3mm thickness. An extensive mesh independence is performed for a bearing with journal speed 3000rpm and eccentricity ratio of 0.5. The best element aspect ratio obtained was 35.966. The solution of the velocity equation coupled with the pressure equation was obtained by SIMPLE algorithm while upwind scheme was used to solve the energy equation. The convergence criteria of  $10^{-4}$  is adopted for all the remaining terms.

### 3. Results and discussion

The static characteristics of plain journal bearing using different nan-lubricants under thermal condition considering cavitation effect are presented and discussed in this article. Different performance parameters regarding the oil film pressure, load carrying capacity, oil film temperature, friction coefficient and side leakage are evaluated at a full range of eccentricity ratios (0.1-0.9), Nano-lubricants with different nanoparticles volume fractions (0.005,0.01,0.02 and 0.03) and other geometric parameters presented in Table (1). Veedol Avalon ISO viscosity dispersed with  $\text{TiO}_2$  and  $\text{Al}_2\text{O}_3$  nano particles with the thermal properties presented in Table 2 was used in the present work. The mathematical model of the present work was validated by comparing the results of the temperature distribution obtained numerically in the present work with that obtained by Ferron et al. (1983) as can be shown in Figure 3.

Type of particles (nm)	$\rho(\text{kg}/\text{m}^3)$	$C_p(\text{J}/\text{kg}\cdot\text{K})$	$K(\text{W}/(\text{m}\cdot\text{K}))$
$\text{TiO}_2$	4230	710	8.4
$\text{Al}_2\text{O}_3$	3970	765	36

**Table 2.** Thermal properties of the nanoparticles

It can be observed from this figure that the results are in a good agreement with maximum deviation of 1.26% due to the different numerical scheme adopted.

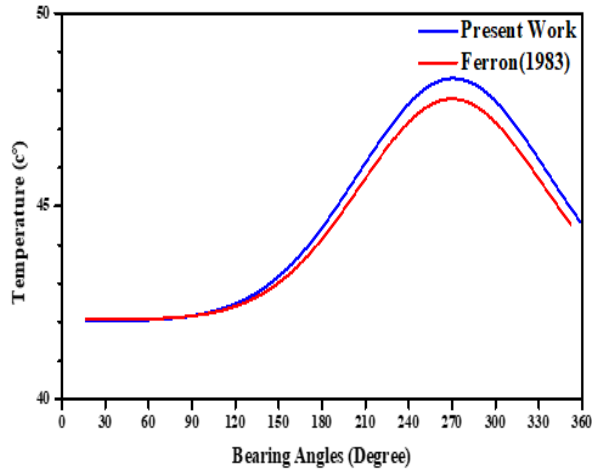


**Fig. 3.** Validation of the temperature distribution.

Figure 3 shows the effect of lubricating the journal bearing with different nano-lubricants dispersed with 3% volume fraction of  $\text{TiO}_2$  and  $\text{Al}_2\text{O}_3$  nanoparticles on the thermal circumferential pressure distribution. This figure clearly shows that the maximum oil film pressure increases by 21.5% when lubricated with the nano-lubricant in comparison with that of pure oil due to the increase of the oil viscosity caused by the addition of the nanoparticles. This figure also depicts that using  $\text{TiO}_2$  nanoparticles give pressure slightly higher than that when using  $\text{Al}_2\text{O}_3$  nanoparticles.

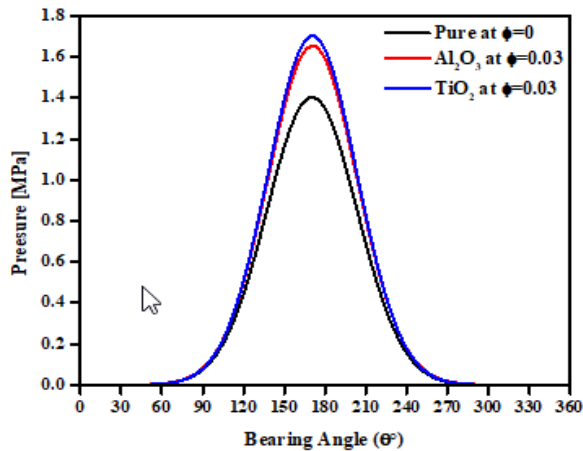


**Fig. 4.** Effect of Nano-lubricant on the pressure distribution ( $l/D=0.5$ ).

The oil film temperature distribution for the bearing works under the same circumstances and is presented in Figure 5. This figure reveals that the oil film temperature increases as the bearing lubricated with oil dispersed by different nanoparticles. This can be attributed to the higher shear stress generated in this case. The oil dispersed with  $\text{TiO}_2$  nanoparticles shows higher oil film temperature due to the tendency of higher aggregation of this material in the base oil.



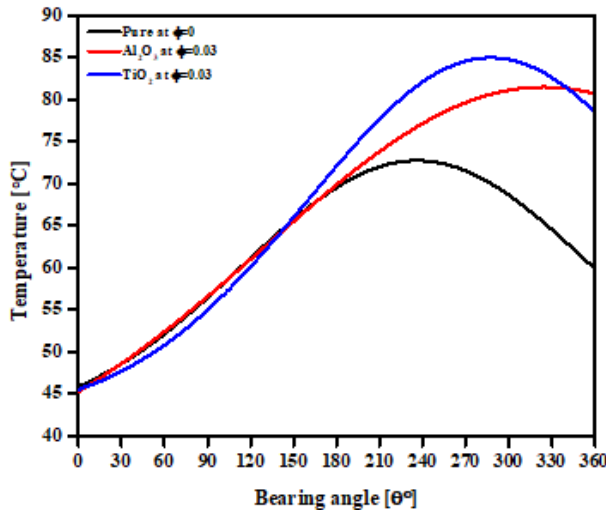


Fig. 5. Effect of nano-lubricant on the oil film temperature distribution.

The maximum oil film pressure for a bearing works at different eccentricity ratios lubricated with oil dispersed with TiO<sub>2</sub> nanoparticles can be shown in Figure 6. It was observed that the maximum oil film pressure increases as the bearing works at higher eccentricity ratios. The increase becomes higher when the bearing lubricated with nano-lubricant that has higher volume fraction of TiO<sub>2</sub> nanoparticles. It can also be seen from this figure that the maximum oil film pressure increases by 20% for the bearing working at 0.7 eccentricity ratio lubricated with nano-lubricant that has 3% of TiO<sub>2</sub> nanoparticles when compared with that lubricated with pure oil. This accompanied with an increase in maximum oil film temperature of about 12.5% and the load carried by the bearing by 9.5% as can be shown from Figures 7 and 8, respectively.

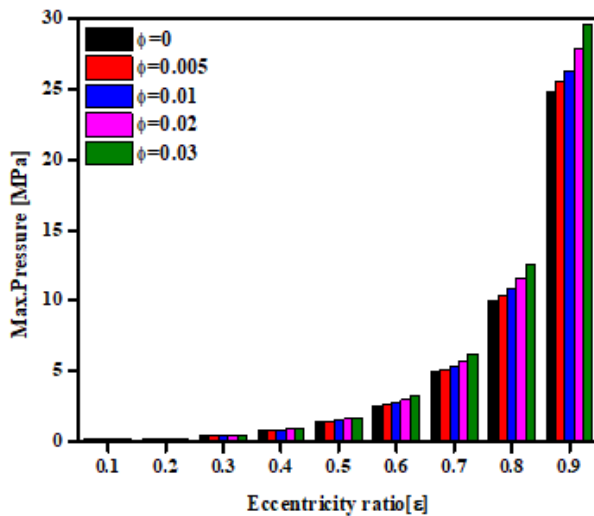


Fig. 6. Maximum oil film pressure vs. eccentricity ratios.

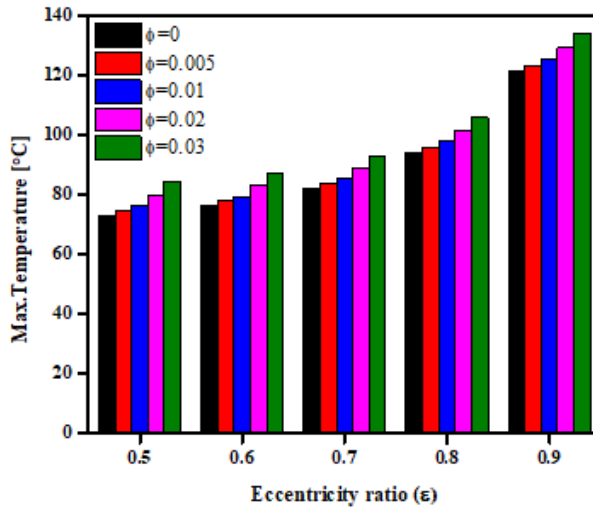


Fig. 7. Maximum oil film temperature vs. eccentricity ratios.

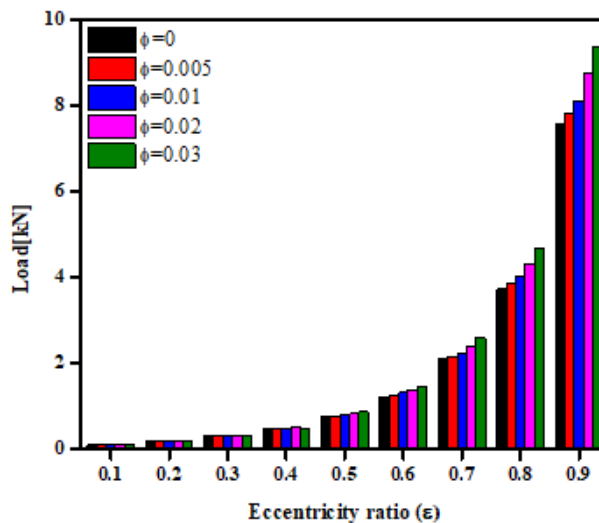


Fig. 8. Load carrying capacity vs. eccentricity ratios.

Figure 9 shows that the load carried by the bearing lubricated with base oil dispersed by 3% of  $\text{TiO}_2$  nanoparticles becomes higher than that lubricated with  $\text{Al}_2\text{O}_3$  Nano particles. This may be explained by the higher aggregation of the  $\text{TiO}_2$  nano-particles which increases the resistance to the flow of lubricant and hence the viscosity of lubricant. The friction force generated at the surface of the bearing working at different eccentricity ratios can be shown in Figure 10. The effect of using nanolubricant with different volume fractions of the  $\text{TiO}_2$  nanoparticles has been considered. It can be seen that the friction force increases when the bearing lubricated with nanolubricants that has higher nanoparticles volume fractions and when it works at higher eccentricity ratios. This can be attributed to the higher shear stress generated in this case.

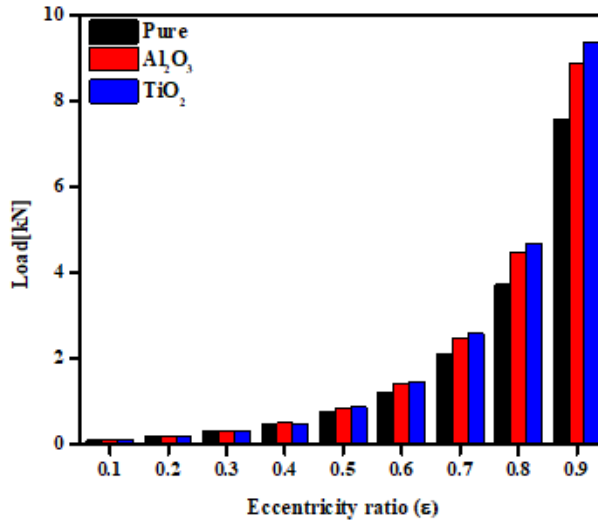


Fig. 9. Load carried by the bearing lubricated with 3% TiO<sub>2</sub> and Al<sub>2</sub>O<sub>3</sub> nano-lubricants.

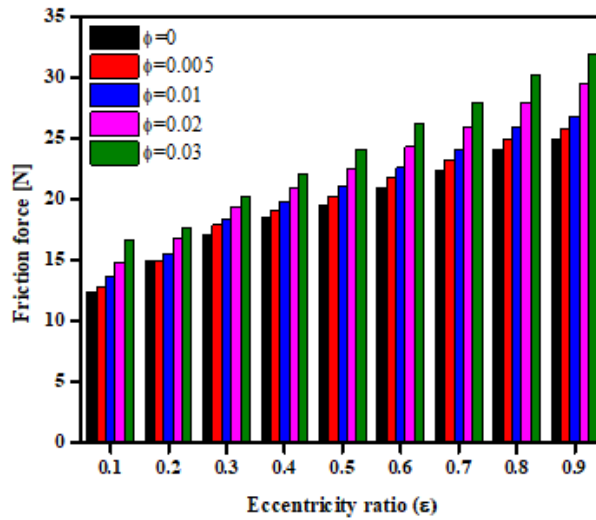


Fig. 10. Friction force vs. eccentricity ratios.

Using TiO<sub>2</sub> Nano-lubricant causes a higher induced friction force than that lubricated with Al<sub>2</sub>O<sub>3</sub> nano-lubricant as illustrated in Figure 11.

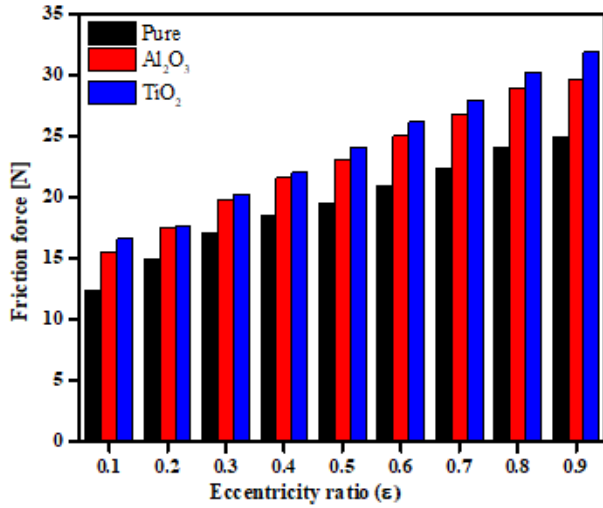


Fig. 11. Attitude angle obtained for a bearing lubricated with 3% TiO<sub>2</sub> and Al<sub>2</sub>O<sub>3</sub> nanoparticles.

However, the coefficient of friction decreases when the bearing works at the same above circumstances as can be shown in Figure 12.

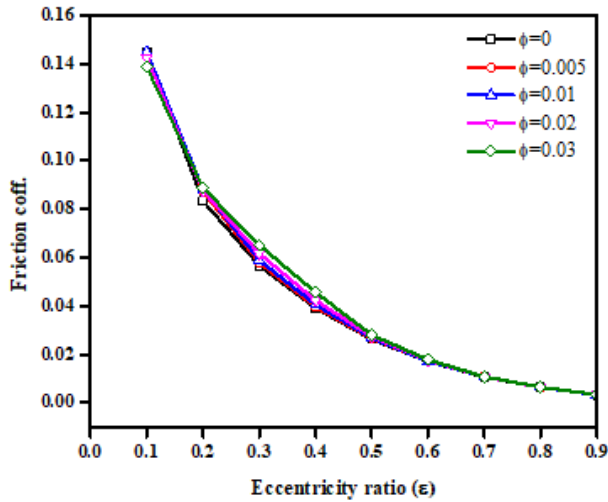


Fig. 12. Friction coefficient vs. eccentricity ratios.

The attitude angel of the bearing decreases as the bearing works at higher eccentricity ratios and lubricated with TiO<sub>2</sub> Nano-lubricant with higher volume fractions of the nanoparticles as can be noticed from Figure 13.

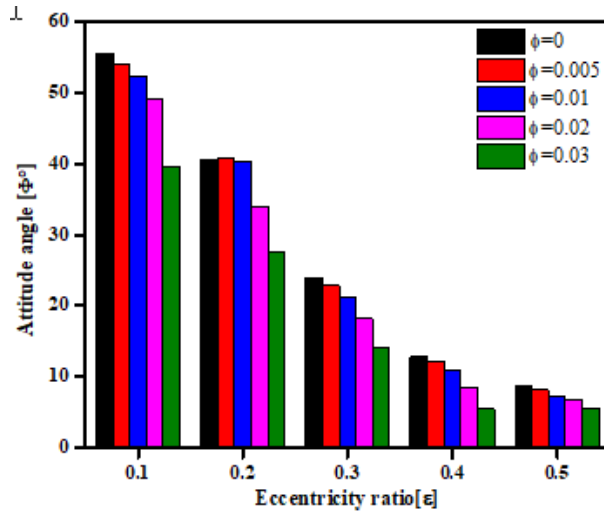


Fig. 13. Attitude angle vs. eccentricity ratio.

This can be explained by the increase in the load carried by the bearing which becomes higher than the friction force generated in this case. A comparison between the attitude angles obtained when aluminum oxide and titanium dioxide nanoparticles added to the base oil can be shown in Figure 14. This figure depicts that using  $\text{TiO}_2$  nanoparticles with base oil leads to a lower attitude angle than that lubricated with  $\text{Al}_2\text{O}_3$  Nano-lubricant for all the range of particle volume fractions.

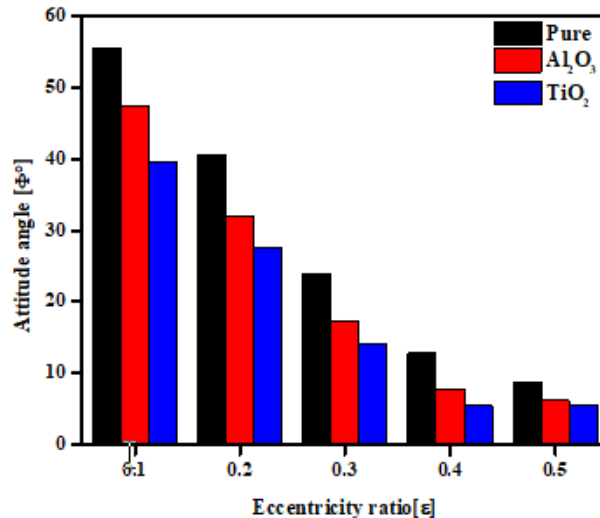


Fig. 14. Comparison between attitude angle obtained for a bearing lubricated with 3%  $\text{TiO}_2$  and  $\text{Al}_2\text{O}_3$  nanoparticles.

Figure 15 shows that the oil flow from both sides of the bearing decreases when the bearing lubricated with Nano-lubricant that has higher volume fraction of  $\text{TiO}_2$  Nano-particles. The decrease becomes higher when using higher volume fraction of such nanoparticles.

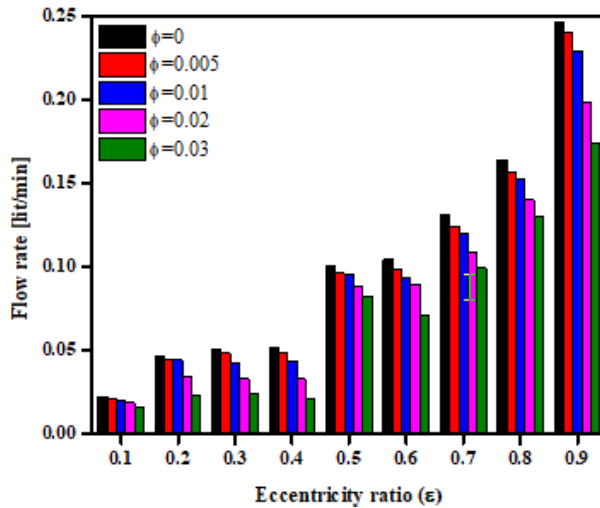


Fig. 15. Flow rate vs. eccentricity ratio.

However, a higher decrease in oil flow rate from both sides of the bearing was observed when the bearing lubricated with TiO<sub>2</sub> Nano-lubricant with 3% of the nanoparticles in comparison with Al<sub>2</sub>O<sub>3</sub> Nano-lubricant as can be shown in Figure 16. Figure 17 depicts the effect of considering cavitation on the circumferential pressure distribution for the bearing lubricated with different nano-lubricants. It can be observed from this figure the oil film pressure increases when the cavitation was considered. This figure also shows that the oil dispersed with TiO<sub>2</sub> nanoparticles has higher oil film pressure than that lubricated with oil dispersed with Al<sub>2</sub>O<sub>3</sub> nanoparticles due to the higher viscosity of the TiO<sub>2</sub> nano-lubricant in comparison with the Al<sub>2</sub>O<sub>3</sub> nano-lubricant.

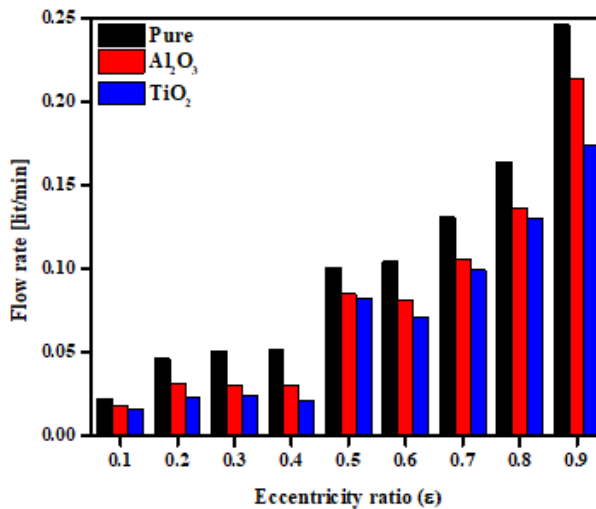
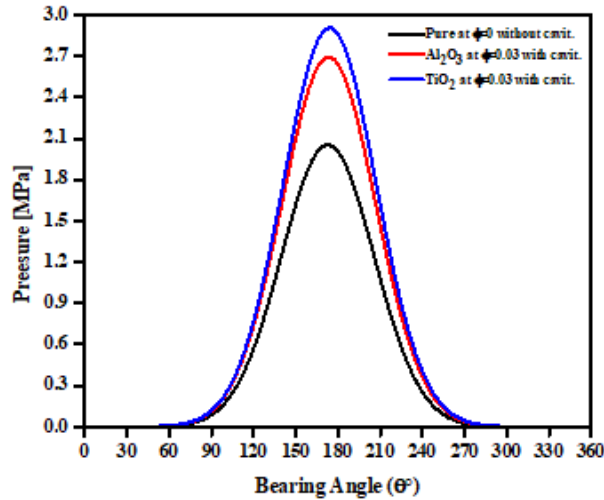
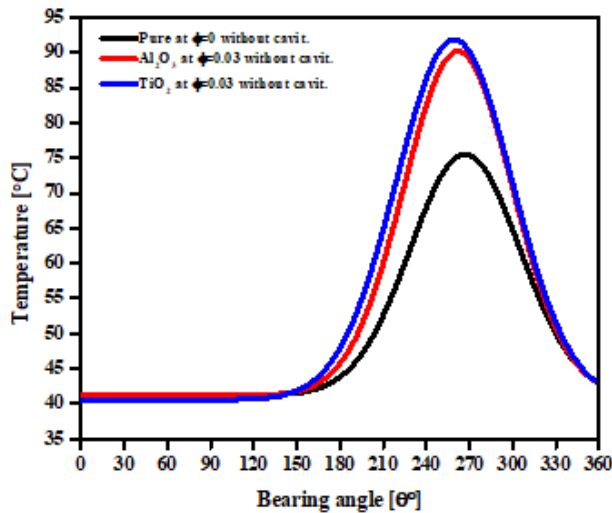


Fig. 16. Comparison between the flow rate obtained for a bearing lubricated with 3% TiO<sub>2</sub> and Al<sub>2</sub>O<sub>3</sub> nanoparticles.



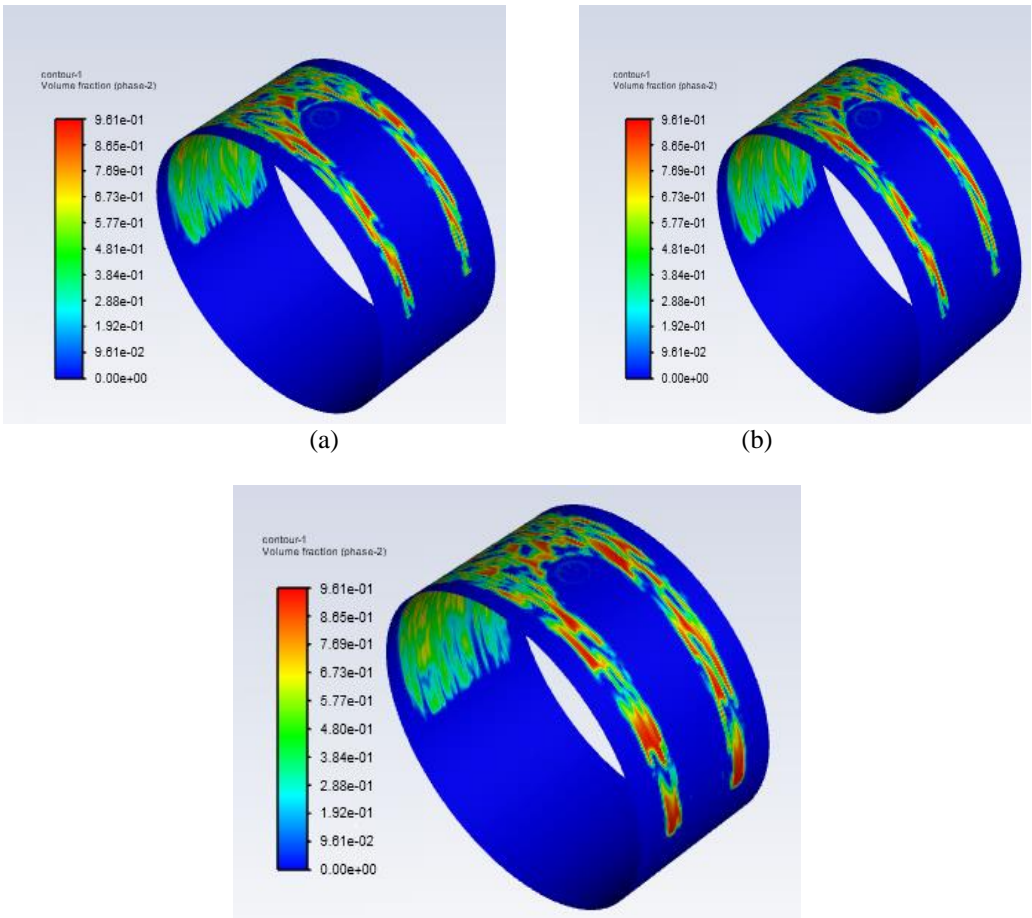
**Fig. 17.** pressure distribution with and without cavitation.

The oil film temperature increases when the cavitation taken into consideration as can be shown from Figure 18. It becomes little higher when the bearing lubricated with  $\text{TiO}_2$  nanolubricant than that lubricated with  $\text{Al}_2\text{O}_3$  nanolubricant.



**Fig. 18.** Temperature distribution with and without cavitation.

Figure 19 a-c shows that the volume fraction of the second phase for a bearing working at eccentricity ratio of 0.5 and journal speed of 3000rpm lubricated with pure and  $\text{TiO}_2$   $\text{Al}_2\text{O}_3$  nanolubricants. It can be observed from this figure that the the nanolubricant has a negligible effect on the volume fraction of the second case. The maximum volume fraction reaches 0.966 and 0.96 for the bearing lubricated with 3%  $\text{TiO}_2$  and  $\text{Al}_2\text{O}_3$  nanolubricant in comparison with that lubricated with pure oil when the volume fraction reaches 0.961.



(c) volume fraction for the bearing with 3% Al<sub>2</sub>O<sub>3</sub> nano-lubricant

**Fig. 19.** Effect of using nanolubricant on volume fraction of the second phase. (a) pure oil (b) 3% TiO<sub>2</sub> Nanolubricant (c) 3% Al<sub>2</sub>O<sub>3</sub> nanolubricant.

**4. Equilibrium position of the journal center**

The equilibrium position is defined as the journal center position at which there is a force balance between the vertical component (y-component) of the hydrodynamic load and the externally applied load on the bearing with the horizontal component of the load (x- component) is equal to zero. It can be obtained by optimizing targets to get zero x-imbalance and y-load equal to the external applied load. The response surface for a bearing lubricated with pure oil and journal speed of 3000rpm shown in Figure 20 is generated using the design of experiment (DOE) data presented in Table 3 which was obtained by guessing the upper and lower bound of the bearing eccentricities and attitude angles within which the solution is expected.



	A	B	C	D	E	F	G	H	I	J	K
1	Name	P1Length (mm)	P2Angle (deg.)	P4-F <sub>x</sub> -op	P5- load op	P6- Fric. Op(N)	P7- side-op kg.s <sup>-1</sup>	P8-f <sub>x</sub> - drag-op (N)	P9-f <sub>y</sub> lift Op (N)	P11-X origin (m)	P12- Y origin (m)
2	1DP8	0.023	31.667	-316.61	672.52	19.761	-0.0014	-312.6	605.88	-12.1μ	-1.96μ
3	2 DP10	0.02861	40.556	-203.86	1074.9	20.625	-0.0013	-198.8	1077.6	-1.8.60μ	-21.73μ
4	3DP4	0.01194	53.88	-89.61	225.51	15.578	-0.00054	-89.37	209.79	-9.649μ	-7.039μ
5	4 DP 7	0.02027	49.44	-90.02	485.14	18.672	-0.0006	-87.16	484.76	-15.407μ	-1.318μ
6	5 DP3	0.00916	27.222	--159.5	177.96	15.36	-0.00057	-159.2	80.284	-4.1932μ	-8.1514μ
7	6 DP5	0.014722	36.111	-114.36	279	16.715	-0.00006	-113.08	258.98	-8.6765μ	-1.189μ
8	7 DP6	0.0175	62.778	6.5562	359.23	17.52	-0.00040	8.1697	364.36	-15.562μ	-8.0052μ
9	8 DP9	0.025833	58.333	61.191	789.8	19.6	-0.00106	65.174	799.5	-21.987μ	-13.562μ
10	9 DP2	0.00638	45	-94.42	118.76	13.609	-0.00036	-94.615	73.106	-4.5176μ	-4.5176μ

**Table 3.** Design point as a result of design of experiments for a bearing lubricated with pure oil.

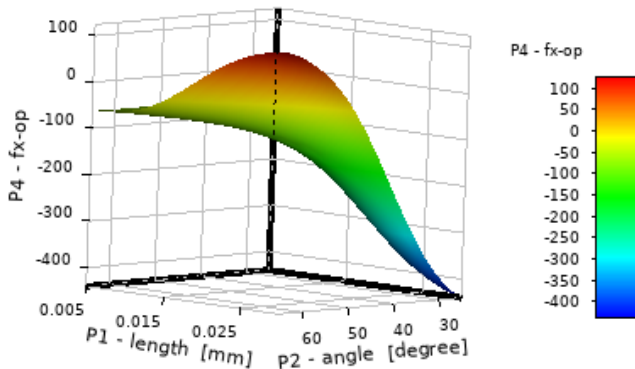


**Fig. 20.** Relation of the bearing x- force component with bearing eccentricity and attitude angle.

Design points and the matrix of experiments is generated by using an optimal space filling design algorithm. The design points are used to generate the response surface which performs the relationship between the eccentricity, attitude angle and the output parameters such as fluid reaction forces. The relation between the X-component of the bearing force, the bearing eccentricity and the attitude angle is clearly shown in Figure 21. The closeness of the data points was confirmed by the goodness of the fit for the data points shown in Figure 23. The optimization constraints and the optimum results obtained for the journal center of the bearing lubricated with pure oil are presented in Figures 21 and 24.

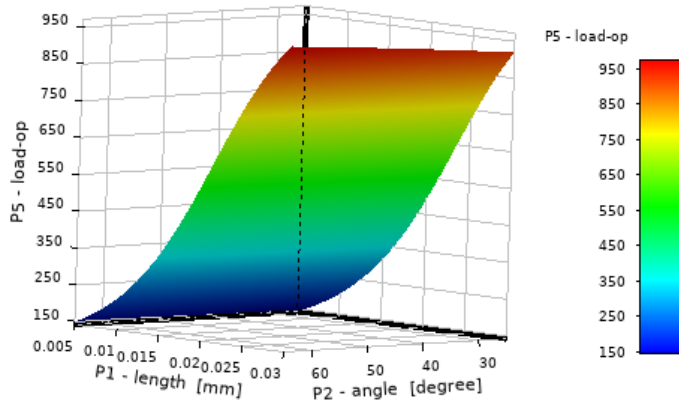


Fig. 21. Relation of Load with eccentricity and attitude angle.

Table of Schematic C4: Optimization					
	A	B	C	D	E
1	Name	Parameter	Objective		
2			Type	Target	Type
3	Seek P5 = 975	P5 - load-op	Seek Target	975	No Constraint
4	Seek P4 = 0	P4 - fx-op	Seek Target	0	No Constraint

Fig. 22. Optimization constraint.

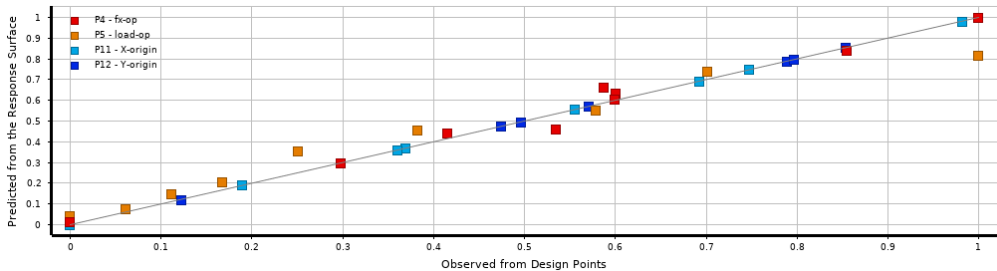


Fig. 23. Goodness of fit.

Table of Schematic C4: Optimization , Candidate Points								
	A	B	C	D	E	F	G	H
1	Reference	Name	P1 - length (mm)	P2 - angle (degree)	P4 - fx-op		P5 - load-op	
2					Parameter Value	Variation from Reference	Parameter Value	Variation from Reference
3	<input type="radio"/>	Candidate Point 1	0.029982	50.834	★ 1.2479	-98.38%	★ 955.47	-0.78%
4	<input type="radio"/>	Candidate Point 2	0.029922	52.776	★ 28.729	-62.72%	★ 956.25	-0.70%
5	<input checked="" type="radio"/>	Candidate Point 3	0.029979	57.162	★ 77.072	0.00%	★ 963	0.00%

Fig. 24. Optimum solution for the journal center (pure oil).

The candidate point with minimum variance represents the optimized solution. Hence, candidate point 3 with eccentricity value of 0.029979mm or  $\epsilon=0.59$ , attitude angle of 57.162°, x-load component of 77.072N and the Y- load component of 963N represents the required

equilibrium point. The optimized journal center for a bearing lubricated with 3% TiO<sub>2</sub> and Al<sub>2</sub>O<sub>3</sub> Nano-lubricants was determined using the above illustrated procedure. The obtained results for these cases are presented in Figures 25 and 26, respectively. It can be concluded from the data in Table 6 that the optimum values of the journal center eccentricity, attitude angle and the X and Y components of the load are 0.029973mm, 58.773°, 16.79N and 1137.1N respectively. Table 7 shows the optimum values of the journal center eccentricity (0.026808), attitude angle (59.771) and the X and Y components of the load -0.22107N and 982.8N.

Table of Schematic C4: Optimization , Candidate Points											
	A	B	C	D	E	F	G		H	I	J
1	Reference	Name	P1 - length (mm)	P2 - angle (degree)	P3 - Mesh Max	P6 - fy-op	P7 - fx-op		P8 - load-op		
2							Parameter Value	Variation from Reference	Parameter Value	Variation from Reference	
3	☉	Candidate Point 1	0.029992	57.239	38.479	-1184.2	★ ★ -0.012678	-100.07%	★ ★ 1134.9	-0.20%	
4	☉	Candidate Point 2	0.029992	58.028	38.508	-1179.7	★ ★ 8.6532	-49.03%	★ ★ 1136.4	-0.06%	
5	☉	Candidate Point 3	0.029973	58.773	38.533	-1174.2	★ ★ 16.977	0.00%	★ ★ 1137.1	0.00%	

Fig. 25. Optimum solution for the journal center (3% TiO<sub>2</sub>).

Table of Schematic C4: Optimization , Candidate Points								
	A	B	C	D	E	F	G	H
1	Reference	Name	P1 - length (mm)	P2 - angle (degree)	P4 - fx-op		P5 - load-op	
2					Parameter Value	Variation from Reference	Parameter Value	Variation from Reference
3	☉	Candidate Point 1	0.029987	63.174	★ ★ 2.7202	1,330.47%	★ ★ 1121.6	14.12%
4	☉	Candidate Point 2	0.028875	61.476	★ ★ -2.2851	-933.69%	★ ★ 1077.6	9.64%
5	☉	Candidate Point 3	0.026808	59.771	★ ★ -0.22107	0.00%	★ ★ 982.8	0.00%

Fig. 26. Optimum solution for the journal center (3% Al<sub>2</sub>O<sub>3</sub>).

## 5. Conclusions

Numerical results obtained in the current paper led to the following conclusions:

1. The maximum oil film pressure and the load carried by the bearing increased when the bearing is lubricated with nano-lubricants. The increase becomes higher when higher particle concentration of the nanoparticles dispersed in the base oil.
2. The oil film temperature slightly increases when the bearing is lubricated with different types of nano-lubricants.
3. The increase in the above-mentioned parameters becomes higher when using TiO<sub>2</sub> nanoparticles rather than Al<sub>2</sub>O<sub>3</sub> nanoparticles.
4. Including the effect of cavitation leading to a higher oil film pressure so that it must be taken into consideration for more reliable results.
5. The optimization technique implemented in the present work shows that the bearing lubricated with Al<sub>2</sub>O<sub>3</sub> shows a lower eccentricity and higher attitude angle than that lubricated with pure oil and TiO<sub>2</sub> Nano-lubricant.

**Acknowledgement:** The authors acknowledge the support of the University of Babylon/College of Engineering/ Mechanical Engineering Department.

## References

- Amit Singla, Paramjit Singh, Abhay Kumar, Arnit Chauhan (2014). Thermo-Hydrodynamic Analysis on Temperature Profile of Circular Journal Bearing using Computational Fluid Dynamics, Proceedings of 2 014 RA ECS UIET, Panjab University Chandigarh.
- Alakhrasing et al. (2015). Thermo-Hydrodynamic Analysis of a Plain Journal Bearing on the Basis of a New Mass Conserving Cavitation Algorithm, *Lubricants*, 3, 256-280
- Ashutosh Kumar, Sashindra Kumar Kakoty, (2017). A Variable Viscosity Approach for the Analysis of Steady State and Dynamic Characteristics of TwoLobe Journal Bearing with TiO<sub>2</sub> Based Nanolubricant, Proceedings of the 2017 Gas Turbine India Conference GTIndia, Bangalore, India.
- Anurag Singh, Neeraj Verma, Aman Chaurasia, Alok Kumar (2020). Effect of TiO<sub>2</sub> additive volume fraction in lubricant oil on the performance of hydrodynamic journal bearing”, IOP Conf. Series: Materials Science and Engineering 802, 012005.
- Anil Dhanola, H. C. Garg (2020). Thermohydrodynamic (THD) Analysis of Journal Bearing Operating with Bio-based Nanolubricants, *Arabian Journal for Science and Engineering*45, pages9127–9144.
- Binu K.G, Shenoy B.S., Rao D.S., Pai R. (2014)., A variable Viscosity Approach for the Evaluation of load Carrying Capacity of oil lubricated Journal Bearing with TiO<sub>2</sub> Nanoparticles as lubricant Additives, *Procedia Materials Science* ,6,1051 – 1067.
- Dhande DY, Pande DW (2016). Numerical analysis of multiphase flow in hydrodynamic journal bearing using CFD coupled Fluid Structure interaction with cavitation. International Conference on Automatic Control and Dynamic Optimization Techniques (ICACDOT), 964-971. IEEE.
- Dhananjay C Katpatal, Atul B Andhare and Pramod M Padole (2019). Performance of nano-bio-lubricants, ISO VG46 oil and its blend with Jatropa oil in statically loaded hydrodynamic plain journal bearing, *Proc IMechE Part J:J Engineering Tribology*,0(0) 1–15 IMechE.
- Fuma Sakai, Masayuki Ochiai, Hiromu Hashimoto (2017). CFD Analysis of Journal Bearing with Oil Supply Groove Considering Two-Phase Flow, The 4th International Conference on Design Engineering and Science, ICDES Aachen, Germany.
- Hamid Sadabadi, Amir Sanati Nezhad, (2020). Nanofluids for Performance Improvement of Heavy Machinery Journal Bearings: A Simulation Study, *Nanomaterials*, 10, 2120.
- J. Ferron, J. Frene, R. Boncompain, (1983). A Study of the Thermohydrodynamic Performance of a Plain Journal Bearing Comparison Between Theory and Experiments, *Transactions of the ASME*, 105,422-428.
- K Prabhakaran Nair, P K Rajendra Kumar, K Sreedhar Babu, (2011). Thermo-hydrodynamic analysis of journal bearing operating under nano-lubricants, Proceedings of the ASME/STLE 2011 International Joint Tribology Conference IJTC2011, Los Angeles, California, US.
- K.G. Binu, B.S. Shenoy, D.S. Rao, R. Pai, (2014). Static characteristics of a fluid film bearing with TiO<sub>2</sub> based nano-lubricant using the modified Krieger–Dougherty viscosity model and couple stress model, *Tribology International*, 75, 69–79.
- Kalakada Sreedhar Babu, K. Prabhakaran Nair, P.K. Rajendrakumar, (2014). Computational analysis of journal bearing operating under lubricant containing Al<sub>2</sub>O<sub>3</sub> and ZnO nanoparticles, *International Journal of Engineering, Science and Technology* 6, 1, 34-42.
- Lin Wang, Zhanhai Han, Guoding Chen and Hua Su, (2017). Thermo-hydrodynamic analysis of large eccentricity hydrodynamic bearings with texture on journal surface”, *Proc IMechE Part C: J Mechanical Engineering Science* 0(0) 1–6.
- Mishra PC, Mukherjee S, Nayak SK, Panda A. (2014)., A brief review on viscosity of nanofluids, *International nano letters*. 4, 4, pp. 109-20.
- Mohammad Yaghoob Abdollahzadeh Jamalabadi, Rezvan Alamian, Wei-Mon Yan, Larry K. B. Li, Sébastien Leveueur and Mostafa Safdari Shadloo (2019). Effects of Nano-particle

- enhanced lubricant films in thermal design of plain journal bearings at high Reynolds numbers, *Symmetry*, 11, 1353
- Qiang Li, Shuo Zhang and Yujun Wang, Wei-Wei Xu, Zhenbo Wang (2018). Investigations of the three-dimensional temperature field of journal bearings considering conjugate heat transfer and cavitation, *Industrial Lubrication and Tribology*.
- R.K. Dang, S.S. Dhimi, D. Goyal, A. Chauhan (2021). Effect of TiO<sub>2</sub> and CuO Based Nanolubricants on the Static Thermal Performance of Circular Journal Bearings, *Tribology in Industry*, doi:10.24874 /ti.995.10.20.02.
- Ramaganesh R, Baskar S, Sriram G, Arumugam S. Ramachandran M. (2020). Finite Element Analysis of a Journal Bearing Lubricated with Nano-lubricants, *FME Transactions*, 48, 476-481.
- R.K. Dang, S.S. Dhimi, D. Goyal, A. Chauhan, (2021). Effect of TiO<sub>2</sub> and CuO Based Nanolubricants on the Static Thermal Performance of Circular Journal Bearings, *Tribology in Industry*, 43, 3.
- Sreedhar Babu Kalakada, Prabhakaran Nair Kumarapillai and Rajendra Kumar P.K, (2015). Static characteristics of thermo-hydrodynamic journal bearing operating under lubricants containing nanoparticles, *Industrial Lubrication and Tribology*, 67, 1, 38–46.
- Solghar AA. (2015). Investigation of nanoparticle additive impacts on thermo-hydrodynamic characteristics of journal bearings. *Proceedings of the Institution of Mechanical Engineers, Part J: Journal of Engineering Tribology*, 229, 10, 1176-86.
- S.R. Suryawanshi, J.T. Pattiwar, (2018). Effect of TiO<sub>2</sub> Nanoparticles Blended with Lubricating Oil on the Tribological Performance of the Journal Bearing, *Tribology in Industry*, 40, 3, 370-391.
- S.R. Suryawanshi, J.T. Pattiwar, (2019). Experimental Study on an Influence of Bearing Geometry and TiO<sub>2</sub> Nanoparticle Additives on the Performance Characteristics of Fluid Film Lubricated Journal Bearing, *Tribology in Industry*, 41, 2, 220-236.
- Tushar P. Gundarneeeyya, D.P. Vakharia, Performance analysis of journal bearing operating on nanolubricants with TiO<sub>2</sub>, CuO and Al<sub>2</sub>O<sub>3</sub> nanoparticles as lubricant additives, *Materials Today: Proceedings*, (Article in press). <https://doi.org/10.1016/j.matpr.2021.02.350>
- Versteeg HK, Malalasekera W. (2007). *An introduction to computational fluid dynamics: the finite volume method*. Pearson, Prentice Hall.
- Vishwanath B. Awati and Ashwini Kengangutti, (2018). Static Characteristics of thermo-hydrodynamic Journal Bearing with Surface Roughness Operating Under Lubricants with Nanoparticles, *Journal of Nanofluids*, 7, 203–209.
- Zuraidah Rasep, Muhammad Noor Afiq Witri Muhammad Yazid (2021). Syahrullail Samion, A study of cavitation effect in a journal bearing using CFD: A case study of engine oil, palm oil and water, *Jurnal Tribologi*, 28, 48-62.